Environ Earth Sci (2016)75:728
DOI 10.1007/s12665-016-5531-7

ORIGINAL ARTICLE

Spatial characterization of the seawater upconing process in a coastal Mediterranean aquifer (Plana de Castellón, Spain): evolution and controls

Olga García-Menéndez[1] · Ignacio Morell[1] · Bruno J. Ballesteros[2] · Arianna Renau-Pruñonosa[1] · Alejandra Renau-Llorens[1] · Mª Vicenta Esteller[3]

Received: 29 May 2015 / Accepted: 3 March 2016

Abstract In this contribution, we describe the formation and evolution of the upconing process in a Mediterranean coastal aquifer. The study area has experienced severe salinization over the last 40 years because of intensive exploitation of groundwater. We used historical and current records of piezometric levels and chloride concentrations to trace the development of the salinization of the aquifer. We defined the 3D shape of the saline wedge from the spatial distribution of chloride concentrations and vertical well logs of electrical conductivity using monitoring network data. Upconing first appeared in the early 90s and has continued until the present day. In this study, we examined the intensity of the upconing process. Dry periods and the associated increases in pumping caused the advance of seawater intrusion. The sharp reduction in groundwater withdrawals over the last 10 years has caused the saline wedge to move backwards, although the ongoing pumping and the climate conditions mean that this retreat is quite slow.

Keywords Seawater intrusion · Upconing · Electrical conductivity vertical logs · Plana Castellón aquifer

✉ Olga García-Menéndez
garciao@uji.es

Ignacio Morell
morell@camn.uji.es

Bruno J. Ballesteros
b.ballesteros@igme.es

Arianna Renau-Pruñonosa
arenau@uji.es

Alejandra Renau-Llorens
erenau@uji.es

Mª Vicenta Esteller
mvestellera@uaemex.mx

1 Coastal Aquifers Research Group, Research Institute for Pesticides and Water, Universitat Jaume I, Avda. Sos Baynat s/n, 12071 Castellón, Spain

2 Coastal Aquifers Research Group, Geological Survey of Spain, C/Cirilo Amorós, 42, 46004 Valencia, Spain

3 Centro Interamericano de Recursos del Agua, Facultad de Ingeniería, Universidad Autónoma del Estado de México, Cerro Coatepec s/n C.U., 50130 Toluca, Mexico

Introduction

Saltwater intrusion is a serious problem for aquifers in many countries in Africa (Steyl and Dennis 2010; Bouderbala 2015), Australia (Werner et al. 2005), Asia (FAO 1997; Liu 2004; Parck et al. 2012; Pratheepa et al. 2015), North America (Cardoso 1993; Barlow and Reichard 2010), and the Caribbean (Morell et al. 1997; Boschetti et al. 2015). In Europe, seawater intrusion affects a large number of coastal aquifers, particularly along the Mediterranean coast of countries such as Spain (Gómez et al. 2003; Renau-Llorens 2010), Italy (Barrocu 2003), Greece (Petalas and Lambrakis 2006), and Turkey (Günay 2003). The problem is mainly the result of inadequate management of water resources resulting from the high density of wells, their proximity to the coastline, and, in some cases, inadequate well design and construction.

Groundwater salinization in coastal aquifers arises from a range of sometimes overlapping factors. In most cases, the predominant process is seawater intrusion that is caused by intensive exploitation. Other associated mechanisms also frequently contribute to salinization, such as regional flows with high salinity (Vengosh et al. 1999), natural mixing processes between seawater and continental water

(Fleury 2005), mobilization of connate water (Lambrakis and Marinos 2003; Stoecker et al. 2013), and urban, agricultural, and industrial discharges (Custodio 2010; Mondal et al. 2011).

Seawater intrusion can generally be categorized into one or more types: horizontal and upward movement of the interface, downward leakage of brackish or saltwater from surface water (such as estuarine environments), or upconing beneath individual wells or well fields (Cheng and Ouazar 2003). Saltwater upconing is a widespread problem in many coastal and inland aquifers around the world (Zakhem and Hafez 2007; Kouzana et al. 2009; Khairy and Janardhana 2013; Rey et al. 2013; Cai et al. 2014) and is a topic of great interest. In general, studies have mainly been restricted to examinations of, and controls on, local saltwater upconing below a pumping well. Numerous analytical and numerical methods have been employed to determine the position of the sharp interface and the critical pumping rate (Chandler and McWorther 1975; Wirojanagud and Charbeneau 1985; Motz 1992; Dagan and Zeitoun 1998; Bower et al. 1999; Garabedian 2013). Reilly et al. (1987) applied a finite element model to determine the maximum permissible discharge rate in an inland aquifer. A number of computer codes have been developed that consider hydrodynamic dispersion in the upconing process and simulate the combined density-dependent flow and salt transport (Diersch et al. 1984; Reilly and Goodman 1987; Zhou et al. 2005; Paster and Dagan 2008). Various studies have demonstrated that numerical modeling is a successful tool for investigating upconing in field applications (Aliewi et al. 2001; Paniconi et al. 2001; Marandi and Vallner 2010; Cai et al. 2014). Because of the challenges associated with making field-based measurements of salt transport dynamics below the pumping well, saltwater upconing research has also been developed at the laboratory scale (Oswald et al. 2002; Werner et al. 2009).

A considerable proportion of the knowledge on the upconing process is based on laboratory and mathematical modeling. To date, however, there have been few field-based studies that report detailed measurements of upconing processes. Recent studies have reported that electrical resistivity profiles can be used to capture and define the shape of the upconing and seawater intrusion (Rey et al. 2013; Kura et al. 2014). However, direct observations of saltwater upconing and additional investigations are needed to give an improved understanding of the 3D nature of seawater upconing in real-world systems (Werner et al. 2013).

In this paper, we have described the evolution of seawater intrusion in the southern part of the Plana de Castellón aquifer over the last 42 years. We used direct field observations [chloride concentration and electrical conductivity (EC) well logs] to define the extent of the upconing process, including its genesis, evolution, and

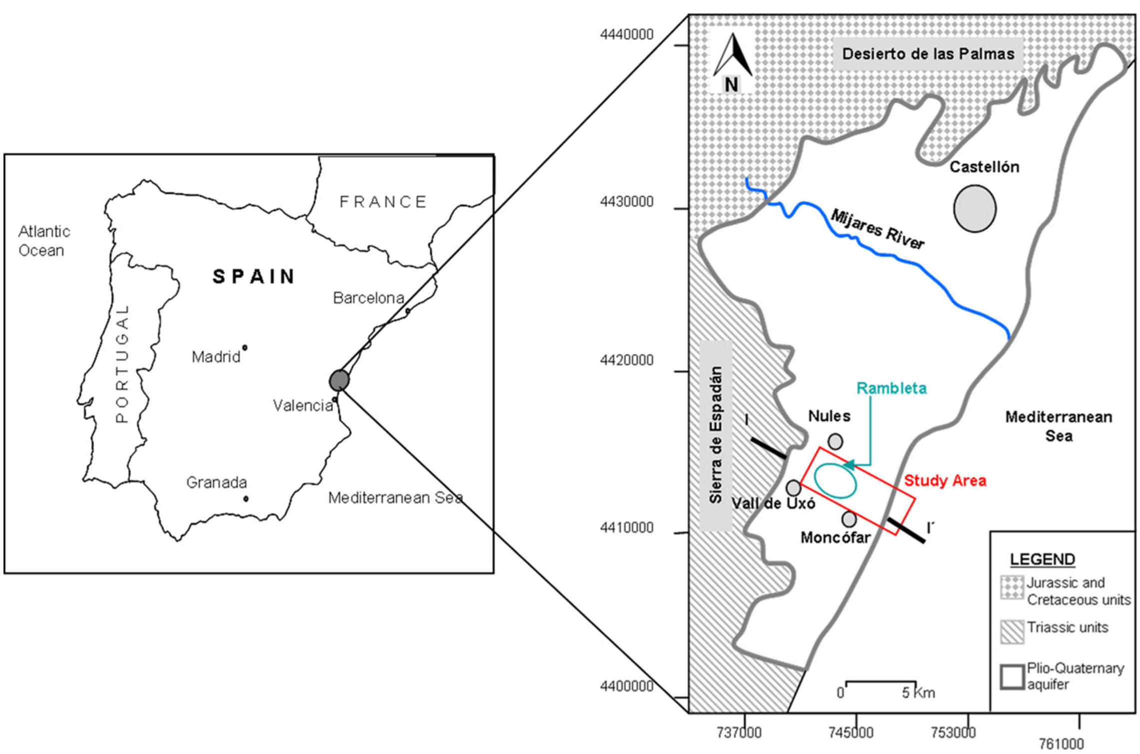

Fig. 1 Situation of the study area

geometry. This approach may be used (a) to establish the relationship between climate conditions, pumping regime, and seawater intrusion; (b) model seawater upconing processes, and (c) to plan management activities, such as artificial recharge, in such an area (García-Menéndez et al. 2015).

Site description and groundwater management

The study area is in the southern part of the Plana de Castellón aquifer on the Spanish Mediterranean coast, where groundwater is extensively exploited (Rambleta Area) (Fig. 1).

The Plana de Castellón is an alluvial plain that covers an area of 490 km^2. There is intensive agricultural, industrial, and tourist activity on the plain, and the area has a population of around 300,000 inhabitants. It is bounded to the north by the Sierra del Desierto de las Palmas, to the southwest by the Sierra del Espadán, and to the east by the Mediterranean Sea.

The average annual precipitation from 1970 to 2014 was 482 mm, with a maximum of 1125 mm observed in 1989, and a minimum of 227 mm observed in 1978. Droughts, defined as a period of 3 consecutive years or more in which the rainfall is below the annual mean, are relatively frequent; extreme rainfall events with more than 200 mm over a 24-h period are also frequent.

There is a permanent watercourse (Mijares River) in the northern half of the Plana de Castellón that supplies water for agriculture in this part of the aquifer. In contrast, groundwater is the main source of urban, agricultural, and industrial water in the southern half of the Plain.

Since the 1960s, the study area has supported significant agricultural activity. Before 1970, the amount of groundwater pumped in the Rambleta was between 4 and 6×10^6 m^3/year. The production wells were shallow (25–40 m) but the flow rates sometimes exceeded 50 L/s. Likewise, there were numerous wells along the coastal strip (north of Moncófar), which provided a further 4×10^6 m^3/year. Additional wells were constructed in the Rambleta to extend the irrigated area and to compensate for the gradual

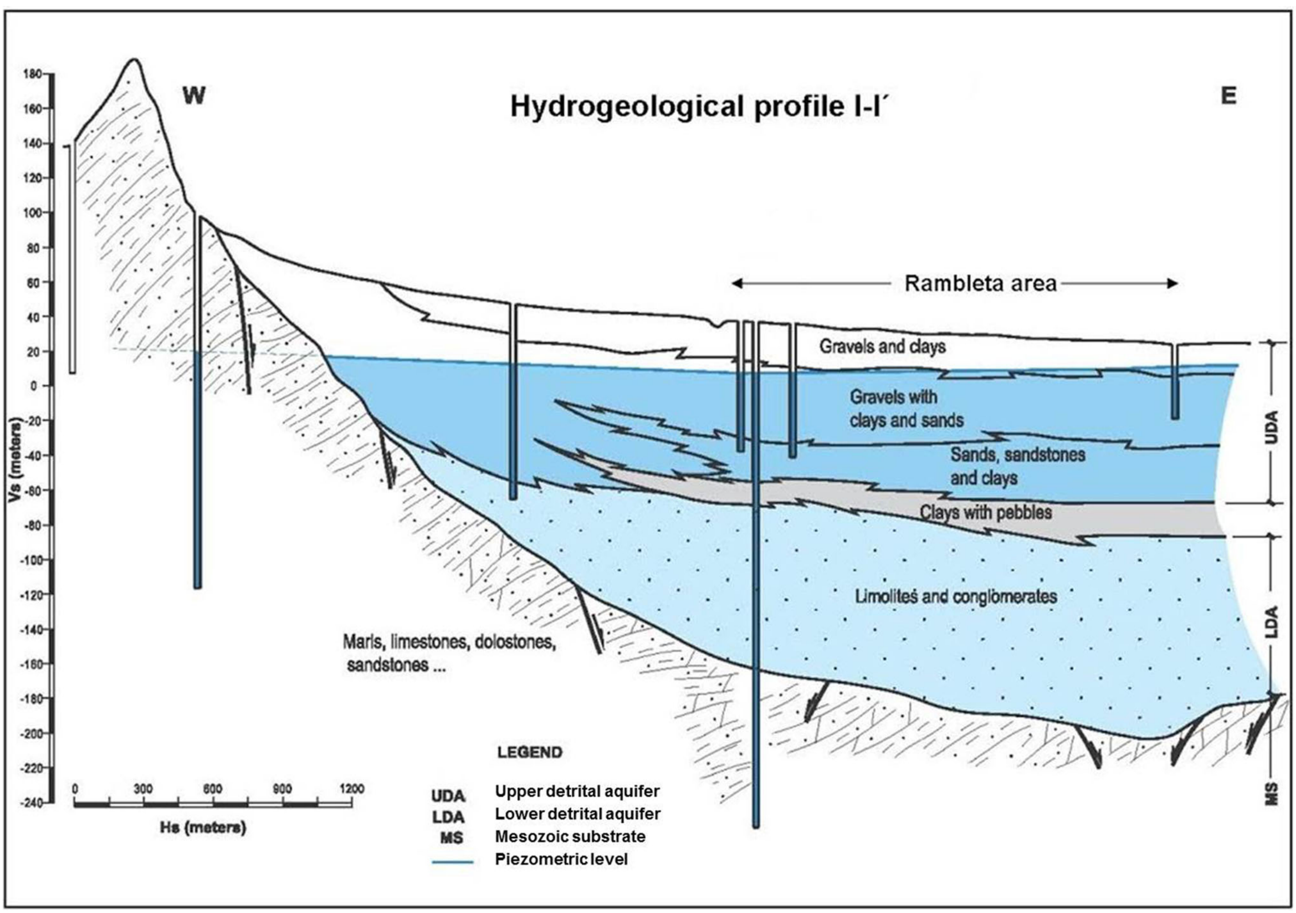

Fig. 2 Hydrogeological cross-section of the Rambleta Area

closure of coastal wells where salinity had increased rapidly. These new wells were generally between 40 and 75 m deep. As a consequence, wells were densely packed into an area of barely 2 km^2, and were only between 100 and 200 m apart. In the mid-nineties, the amount of groundwater pumped for agriculture in this area increased to 21 $\times$ 10^6 m^3/year and an extra 3 $\times$ 10^6 m^3/year was abstracted to supply a drinking water plant.

As detailed below, this intensive exploitation provoked a widespread drop in the piezometric surface and encouraged the progression of the saline front. Even now, there is ongoing degradation of groundwater quality and almost all of the wells in the coastal area and many of the wells in the Rambleta have been abandoned. As a result, some of the production, including the drinking water supply, has been moved to adjacent aquifers.

The groundwater pumping has now decreased to around 14 $\times$ 106 m^3/year, almost half of the peak production, for various reasons. The irrigation system has been modernized from a flooding to a drip-feed system, because of which the unit application rate has decreased from 8500 to 5200 m^3/hectare/year; infrastructure was constructed; 15 % of the croplands were abandoned, and treated wastewater, amounting to 2.5 $\times$ 10^6 m^3/year, has been incorporated into the irrigation network.

Geological and hydrogeological characterization

A tecto-sedimentary plan of the study area has been established (Fig. 2) from the results of geophysical surveys and lithological columns of existing boreholes (Morell et al. 2014). There are four lithological series, including two detrital Plioquaternary formations, an upper detrital aquifer (UDA), and a lower detrital aquifer (LDA). They are separated by a layer of clay with gravels.

The UDA formation is 85-m thick and comprises polygenic gravels, clays, sands, and sandstones. Permeability is due to intergranular porosity (2–8 %) and transmissivity values are $\sim$300 m^2/day, with a maximum of 1000 m^2/day. The highest yields are from the wells in the Rambleta Area, which have specific flows of between 6 and

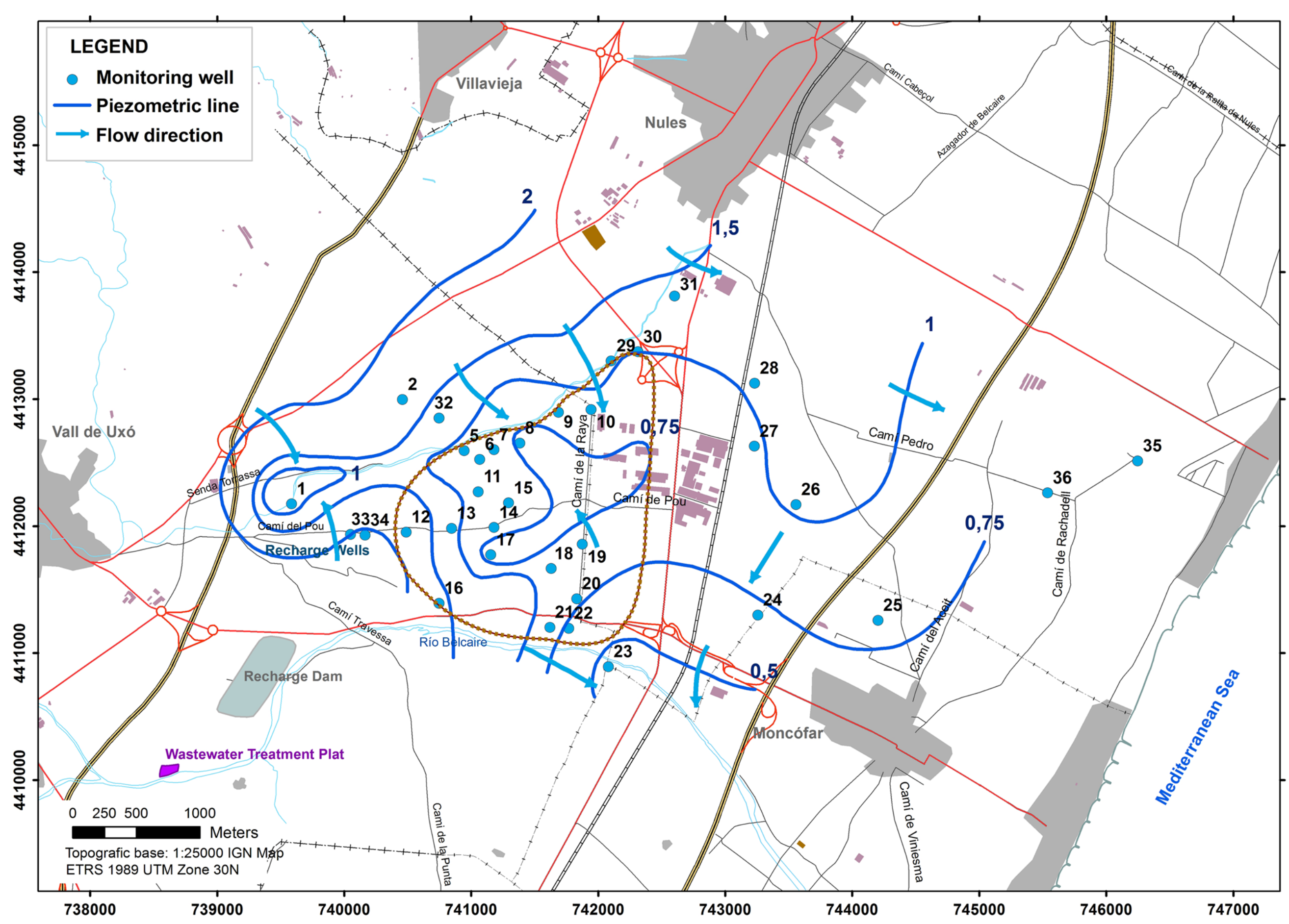

Fig. 3 Piezometric map (October 2012). The Rambleta Area is *circled* in *brown*

10 L/s/m. The impermeable base is 20-m thick, and comprises a layer of clays with gravels.

The LDA is composed of limolites and clays with layers of sandstones and polygenic conglomerates. Permeability is attributable to the porosity of the scarce sand and conglomerate layers, so this formation is of less hydrogeological importance than the UDA. The LDA is between 50 and 100 m thick, increases towards the coast, and is sometimes absent where the Mesozoic substratum (MS) rises closer to the ground surface because of the NNE–SSW direction fault (parallel to the coastline).

The MS underlies all the above-mentioned formations. It comprises limestones, marls, dolostones (Muschelkalk facies), orthoquartzitic sandstone and limolites (Buntsandstein facies), and marls with gypsum (Keuper facies), which have undergone intense folding and fracturing. In general, they form a paleorelief that has been fossilized by the overlying sediments. The MS formation includes two aquifers corresponding to Muschelkalk dolostones and Buntsandstein sandstone. In these settings, there may be hydraulic connections with the overlying permeable formations.

Materials and methods

Detailed geological knowledge of the Rambleta Area was assembled from a comprehensive inventory of wells, boreholes, and lithological columns, and from measurements of electrical resistivity tomography, collected in several campaigns.

The general characteristics (coordinates, elevation, depth, design features, etc.) of 115 wells were recorded, from which 33 lithological columns were compiled.

A computer (Terrameter SAS4000 ABEM) with an imaging system (LUND) and an interelectrode spacing of

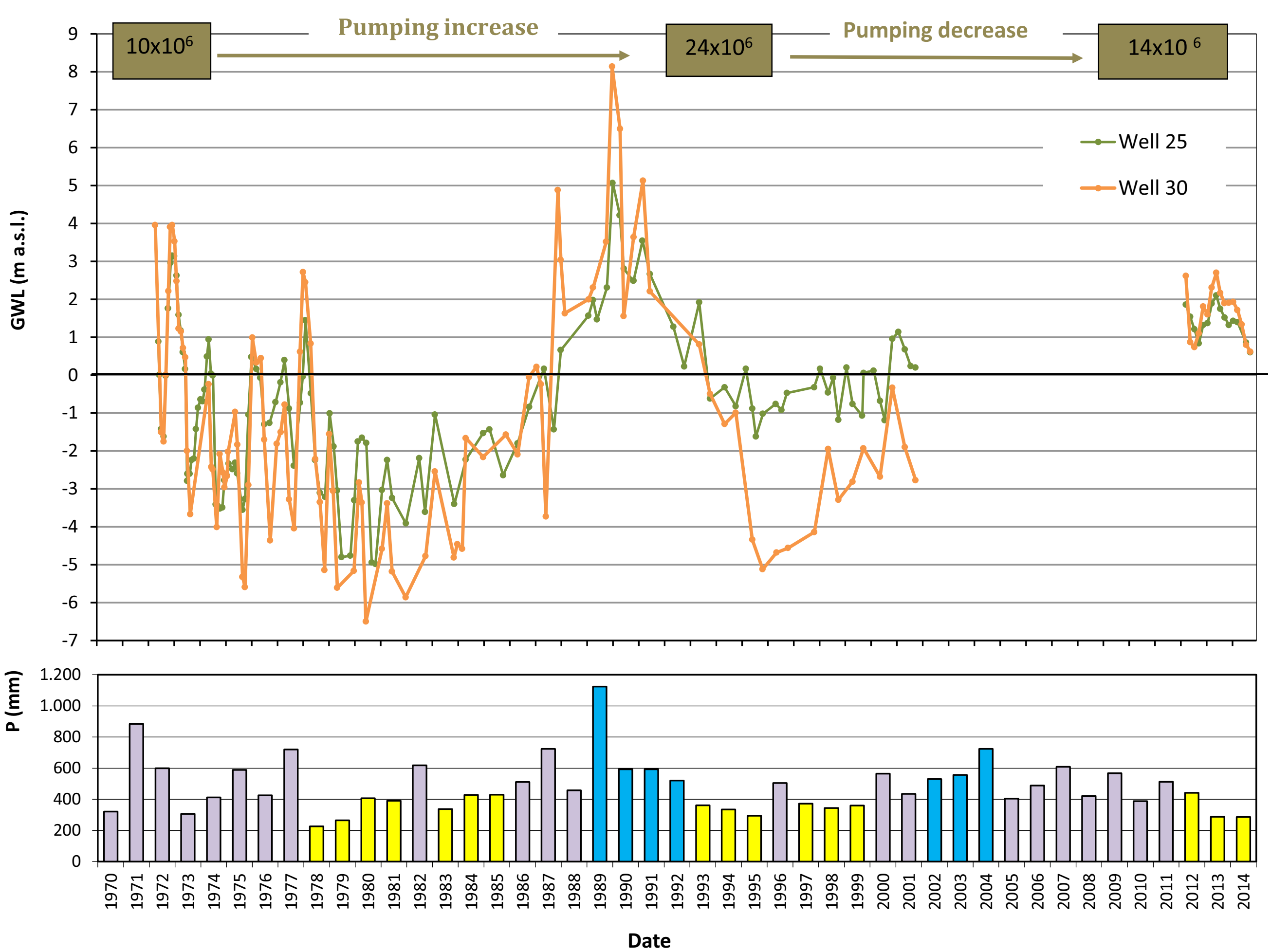

Fig. 4 Evolution of the piezometric level (Wells 25 and 30). Precipitation (*below*): wet period (*blue*), dry period (*yellow*) and medium precipitation (*gray*). At the *top*, exploitation values are detailed in m^3/year

15 was used for the geophysical surveys. A geophysical inversion software package (RES2DINV v.3.46b) was used to convert the field data, and the robust and constrain inversion algorithm was used to obtain the resistivity profiles. We produced a total of six profiles, four of which were 1200-m long and two that were 900-m. Additional induced polarization measures were carried out in four of the profiles.

Historical data of piezometric levels and chloride concentrations were obtained from the monitoring network of the Geological Survey of Spain (IGME), which was initiated in the early 1970s. In 2001, the management of monitoring networks was transferred to the Environment Ministry and the Júcar River Basin Authority (CHJ). The CHJ designed a new piezometric monitoring network that has been operational since 2001. It has fewer piezometers, and no data have been collected in our study area since 2001. In addition, the CHJ established a specific network for monitoring seawater intrusion in coastal aquifers in 2005, and aquifers have been biannually monitored for chlorides, nitrates, bicarbonates, EC, and temperature. However, there is no data for the period from 2001 to 2005.

In view of the sparse information available, we designed a monitoring network consisting of 34 points in the study area (Fig. 3), and carried out bimonthly monitoring between April 2012 and October 2014 (16 surveys). The monitoring network is made up of irrigation wells, 20 of which are now abandoned. The wells were constructed to a standard design. They penetrate fully into the aquifer, with the exception of the dug wells near the coast (more shallow, less than 25-m depth), are totally screened and have large diameters (1–3 m).

An electronic water level meter (Seba-Hydrometre-D-8950 Kaufbeuren), with a 200-m gradient measurement tape and an accuracy of 1 cm, was used to measure the water levels. The measurement reference point (MRP) elevations of the monitoring wells, normally the rim, were measured with a differential GPS (Thimp) with an accuracy of 1 cm and a theodolite (Nikon AP-5). We used the geodetic vertices of the National Geodetic Network of the Geographic Survey of Spain (IGN) for the altimeter

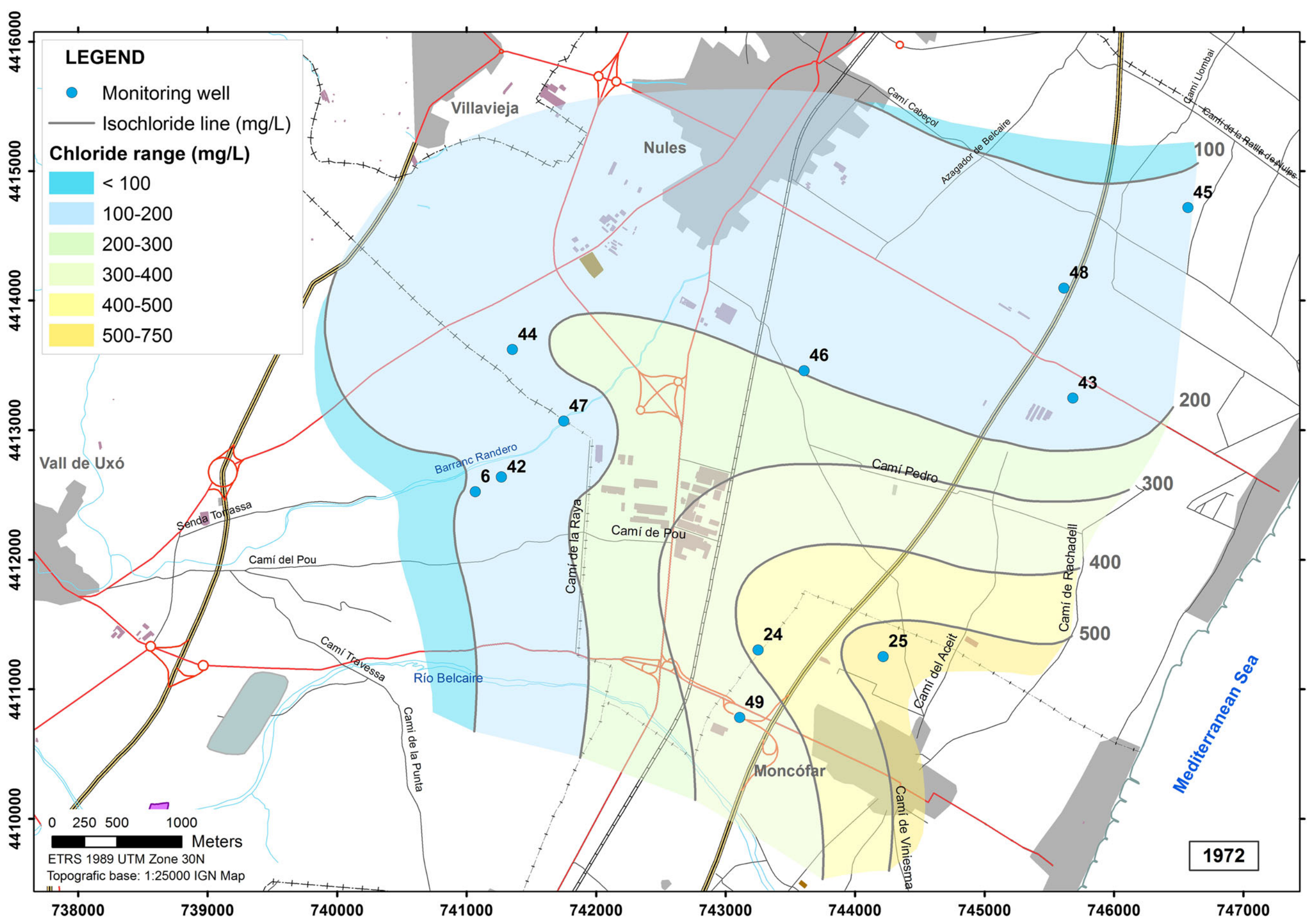

Fig. 5 Spatial distribution of chloride concentrations in June 1972

settings. Altitudes of geodetic vertices, obtained from high precision leveling lines (IGN), are referred to mean sea level, defined by the main tide gauge of Alicante port. The depth of the groundwater (m) was always measured from the MRP, and the groundwater levels in meters above sea level (m a.s.l.) were then calculated by subtracting the depth of the water level (m) from the surface elevation (m a.s.l.) of the MRP. The salinity values of the groundwater ranged from 1500 to 4500 µS/cm, and the water densities were below 1000.77 kg/m^3 and did not vary significantly. As such, piezometric corrections were not needed because the error associated with the head measurements was generally less than 0.02 (Post et al. 2007).

Water was sampled from a depth of 5 m below the water level with a discrete interval sampler (Solinst 425) and a controlled opening mechanism. EC, pH, and temperature were recorded in situ with a waterproof pH/conductivity/temperature portable meter (Eutech Instruments PC650). Further samples for chloride analysis were stored in polyethylene bottles. Chloride concentrations were determined by titration with silver nitrate, following the method of Mohr. Vertical measurements of EC and temperature were logged bimonthly in all monitoring wells from December 2012 to October 2014 using a 100-m long well logger (TLC Solinst).

Most of the historical data were from samples collected by pumping, which means that there is a difference between the historical and the recent data. Samples from pumping describe the quality of the part of the aquifer that is influenced by the pump, while samples from a depth of 5 m below the water level describe the quality at that specific depth. This can, in some cases, lead to quantitative differences in the chloride concentrations. In this study, the differences were not sufficient to significantly alter the trends in salinity.

The groundwater contour lines and the chloride concentration contour maps were created using geographic information system (GIS) software (ArcGIS 10.1). Contour maps were generated using the spatial interpolation Kriging method, which was included in the GIS software

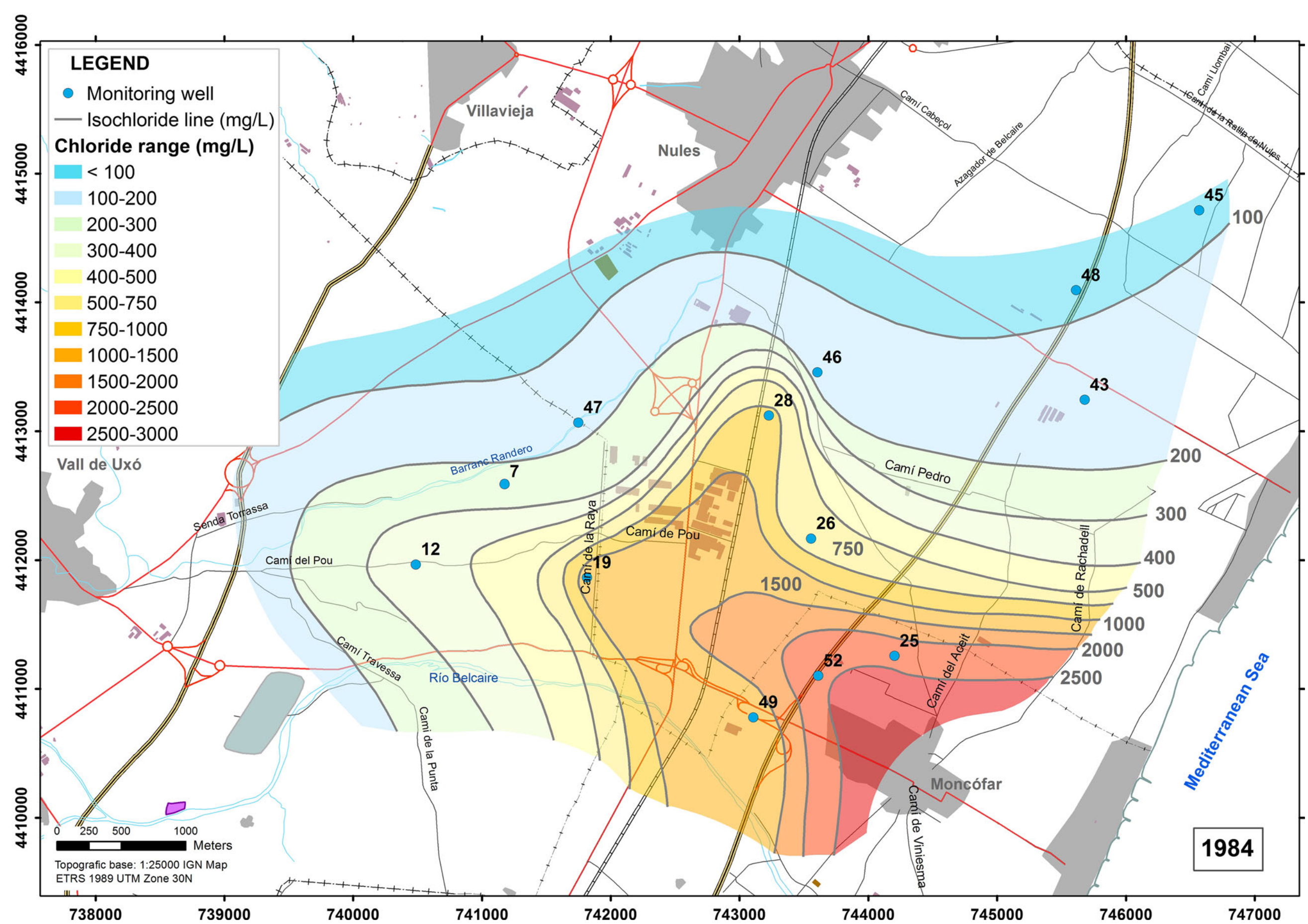

Fig. 6 Spatial distribution of chloride concentrations in June 1984

(ArcToolbox), and then were modified to take account of hydrogeological criteria using ArcMap editing tools. A 1:25,000 IGN map was used as the topographic base.

Results and discussion

Piezometric behavior

Because of the groundwater exploitation and climate, piezometric levels have changed markedly since 1970. These changes are reflected in the piezometric history of Wells 25 and 30 (Fig. 4), which are located close to the coastline and in the Rambleta Area, respectively. The trend in both cases is quite similar but the amplitude of the oscillations differ. Both wells show periods of rising and falling levels, which correspond quite well with wet and dry periods, respectively, and also with the exploitation regime. The influence of climate and exploitation generally overlap. They may have different weights and may vary, depending on the length of the dry or wet periods and the pumping intensity.

Piezometric levels were clearly below sea level between 1973 and 1987 and also from 1993 to 2001, with some measurements dropping to 5 m below sea level (b.s.l.). In contrast, the highest levels were from 1972 to 1973 and from 1987 to 1993, when they exceeded 4 m a.s.l. In the current period (from 2012 to 2014), the depth to the water level is above sea level, and is between 0.5 and 3 m a.s.l.

The piezometric contour line (Fig. 3) shows two depressions, one in the west and the other in the central zone. These two depressions alter the natural groundwater flow direction from the western boundary towards the Mediterranean Sea.

Hydrochemical behavior

There are two main hydrogeochemical water types in the study area: the calcium chloride type and the calcium–magnesium sulfate type. The chloride water corresponds

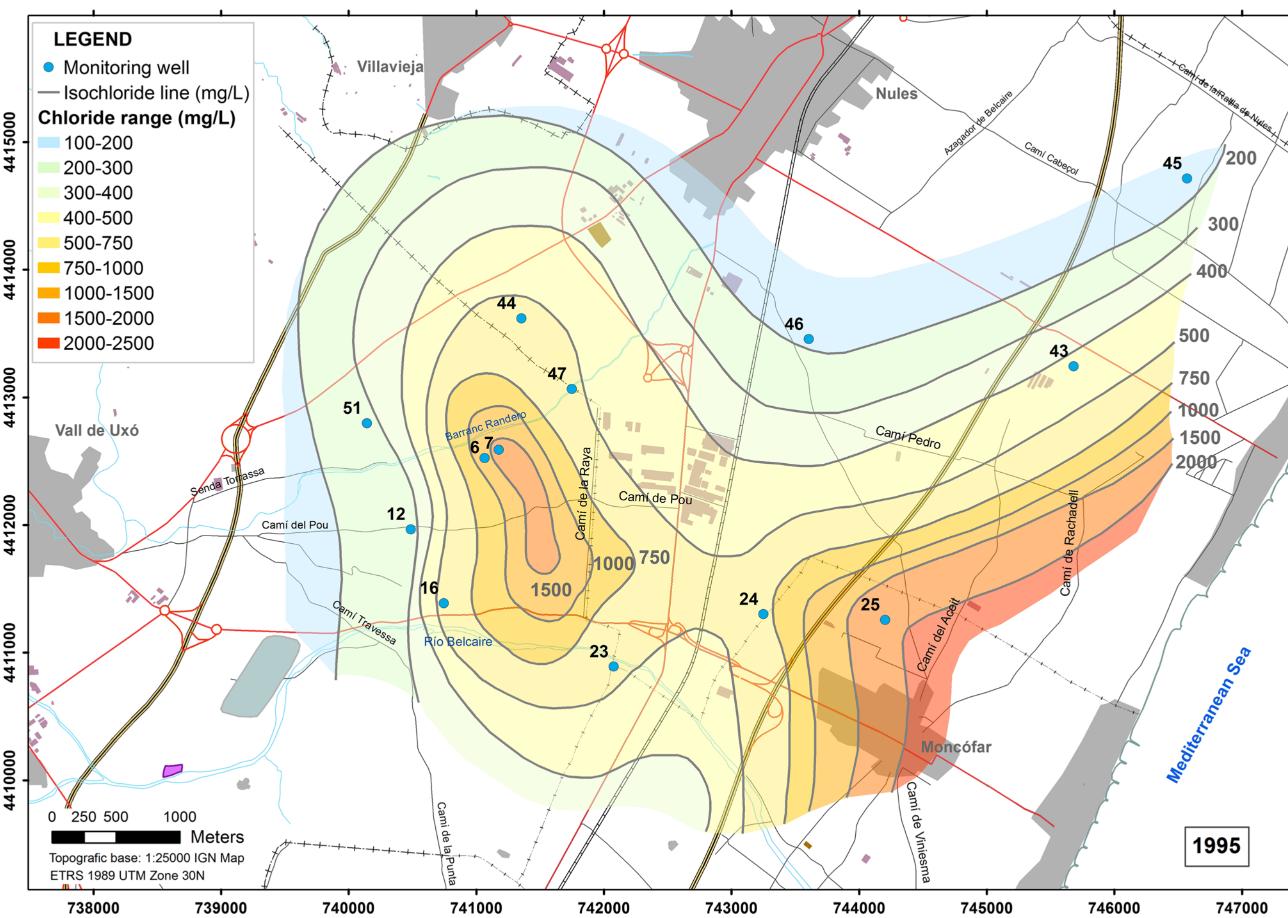

Fig. 7 Spatial distribution of chloride concentrations in October 1995

with a mixture of freshwater and seawater as a consequence of seawater intrusion, while the sulfate water is associated with regional flows from the Triassic limestones and dolomites of the Mesozoic substrate (Fidelibus et al. 1992; Escrig et al. 1993; Giménez 1994; Morell et al. 1996; Giménez and Morell 2008; Renau-Llorens 2010; Giménez-Forcada and Vega-Alegre 2015).

In the early 1970s, salinization followed the usual pattern of aquifers influenced by seawater intrusion, with a progressive decrease from the coast towards the interior. However, in 1972 (Fig. 5), a zone with chloride concentrations above 500 mg/L was visible 2 km inland (north of Moncófar). At this time, the chloride concentrations in the Rambleta Area were less than 200 mg/L.

In the Moncófar area, the water quality in the wells deteriorated significantly, so that, by 1984, the chloride concentrations exceeded 2000 mg/L (Fig. 6). In addition, concentrations above 500 mg/L were detected 5 km inland, thereby influencing the eastern part of the Rambleta (Well 19).

In 1995, concentrations were still very high, but the chloride concentrations had dropped to below 2000 mg/L in the north of Moncófar (Fig. 7), and an area appeared between this area and the Rambleta in which the concentrations were below 750 mg/L. In contrast, concentrations were above 1500 mg/L in the Rambleta Area, resulting in the formation of a saline cone with a surface area of about 5 km^2 and concentrations exceeding 500 mg/L.

An overall improvement in quality was noticed in 2004 (Fig. 8). This improvement was the result of the wet period from 2002 to 2004 and a drastic modification in the management model. The increase in groundwater salinity (Fig. 7) led to a remarkable reduction in groundwater pumping in the Rambleta Area and wells in Moncófar were abandoned. In the latter area, concentrations were around 400 mg/L, and a 2-km wide zone of fresh water appeared between Moncófar and Rambleta. The upconing area with chloride concentrations exceeding 500 mg/L and maximum concentrations of around 1000 mg/L across an area of about 8 km^2

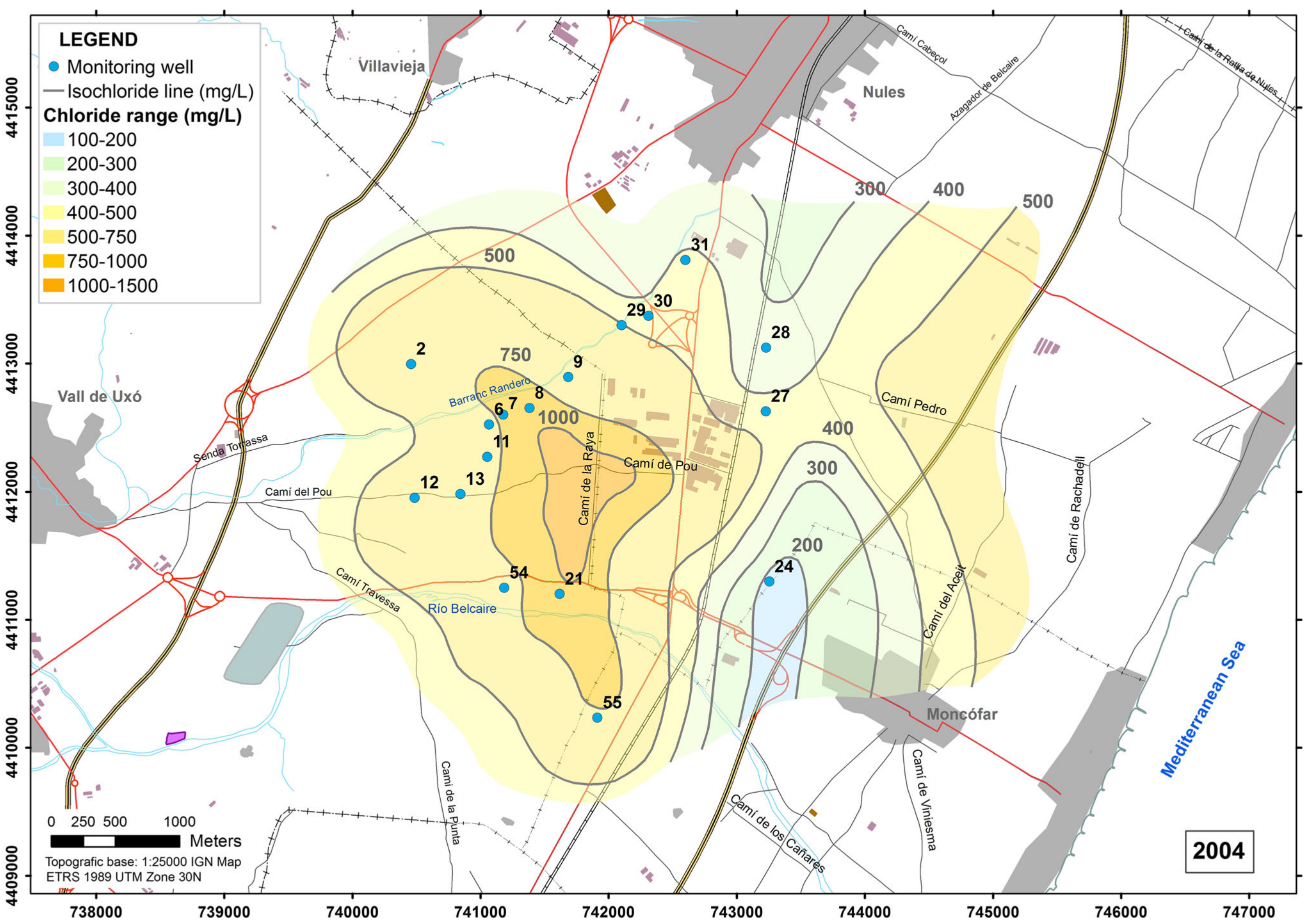

Fig. 8 Spatial distribution of chloride concentrations in September 2004

remained in the Rambleta, but it shifted slightly to the east.

In 2012 (Fig. 9) the upconing still persisted over a wide area, and had chloride concentrations ranging from more than 500 mg/L to slightly more than 750 mg/L. Even though the concentrations were lower than those recorded previously, the salinization was still severe. At the same time, the freshwater zone in the north of Moncófar became wider, with concentrations between 100 and 300 mg/L.

Figure 10 shows changes in the chloride concentrations in four monitoring wells from 1972 to 2014. In Well 25, which was closest to the coast, the concentration exceeded 2700 mg/L in 1983 and since then has gradually dropped to the current value of around 250 mg/L. In contrast, in Wells 2, 7, and 12, situated in the Rambleta Area, the salinity has increased from initial values of around 250 mg/L (1982) to about 600 mg/L. While there was a notable increase in salinization in Well 7 in the middle part of Rambleta in the 1990s, the degree of salinization has remained practically constant in Wells 2 and 12 on the western boundary of the Rambleta.

Characterization of the saline upconing

The three-dimensional (3D) shape of the seawater intrusion was defined precisely using information from the vertical EC logs from the monitoring wells. We used isoconductivity contour maps from December 2013 for depths of 0, 5, 10 and 15 m b.s.l. to develop the 3D picture of the hydrochemical stratification caused by the upconing. The high correlation between chloride concentrations and EC shows that this is a suitable approach for defining the distribution of seawater salinity. The coefficient of determination is 0.74 when pairs of values from wells with low mineralization and the sulfate groundwater type are included. However, if we only consider the chloride type, which dominates in the upconing area, the coefficient rises to 0.95 (Fig. 11).

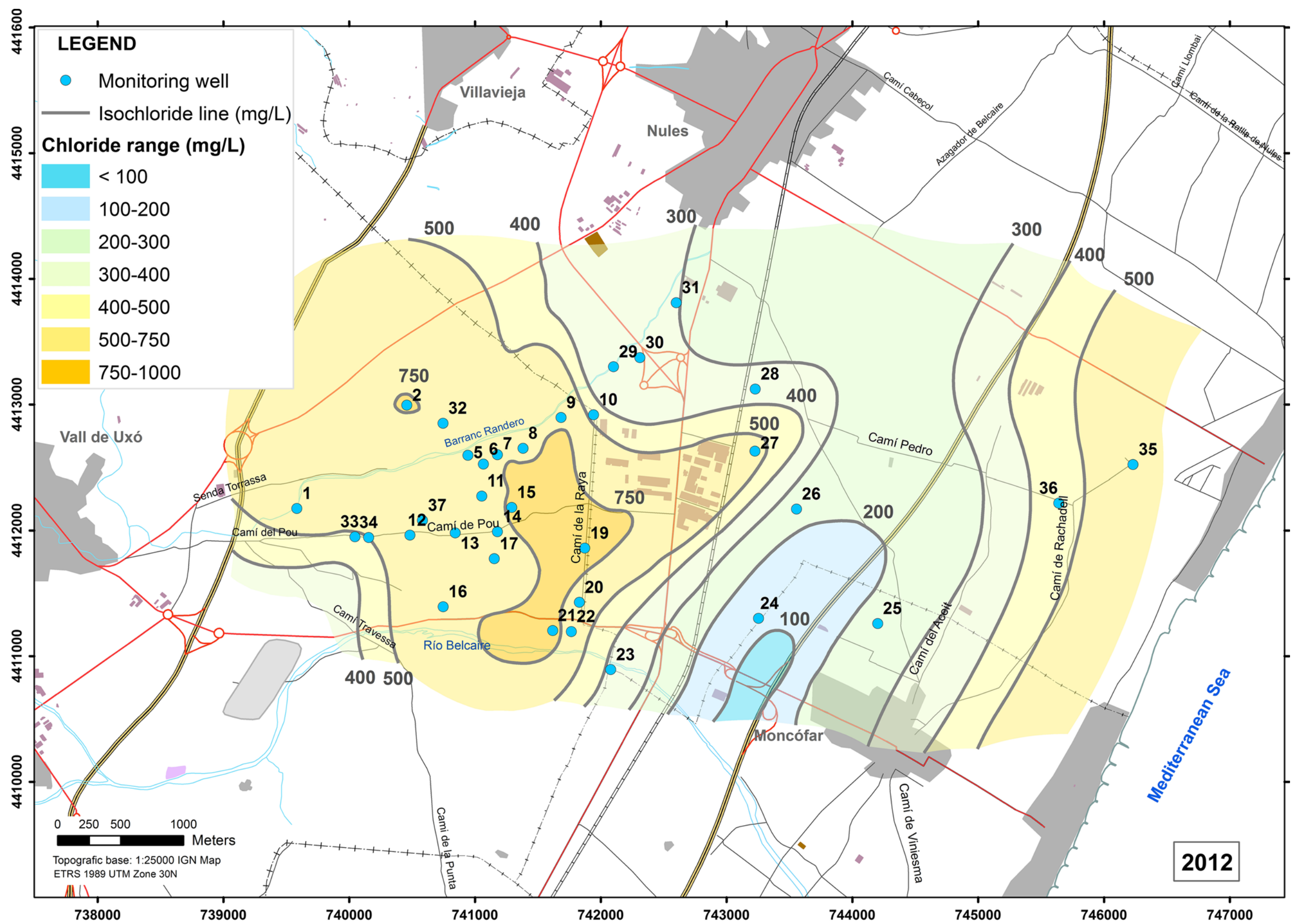

Fig. 9 Spatial distribution of chloride concentrations in October of 2012

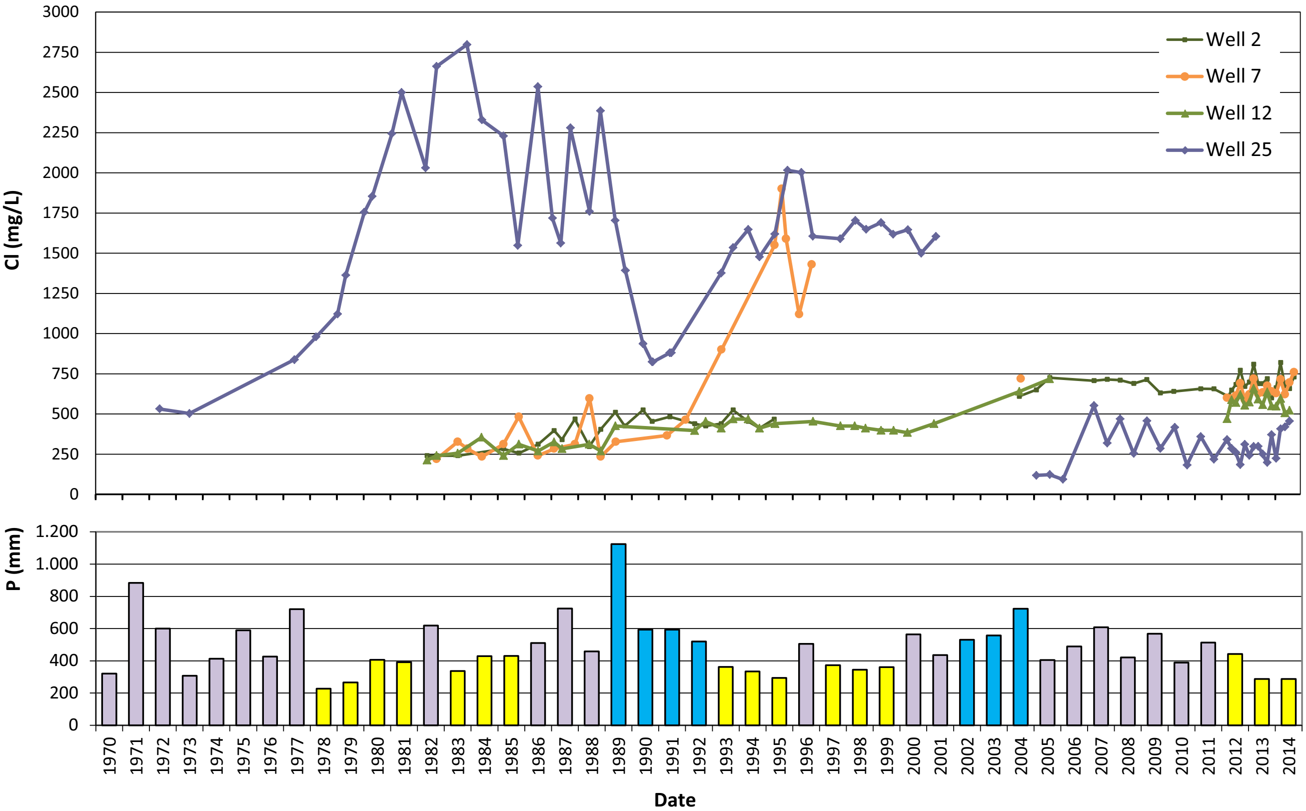

Fig. 10 Evolution of the chloride concentrations (Wells 2, 7 12 y 25) and precipitation (*below*): wet period (*blue*), dry period (*yellow*) and medium precipitation (*grey*)

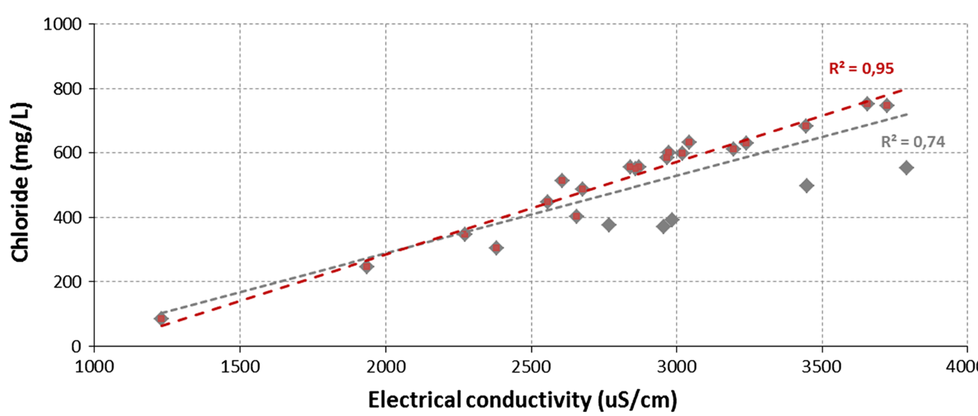

Fig. 11 Relationship between EC and chloride concentrations (December 2013)

At 0 m a.s.l. (Fig. 12), the salinities were highest, and above 3500 µS/cm, in the coastal strip and in the Rambleta area. There is a body of fresh water with EC values of 1000 to 2000 µS/cm between these two zones that clearly separates the area of lateral movement of the intrusion (coastal area) and the upconing area.

At 5 m b.s.l. (Fig. 13) the distribution of salinity in the Rambleta is quite similar to that at 0 m a.s.l. but the

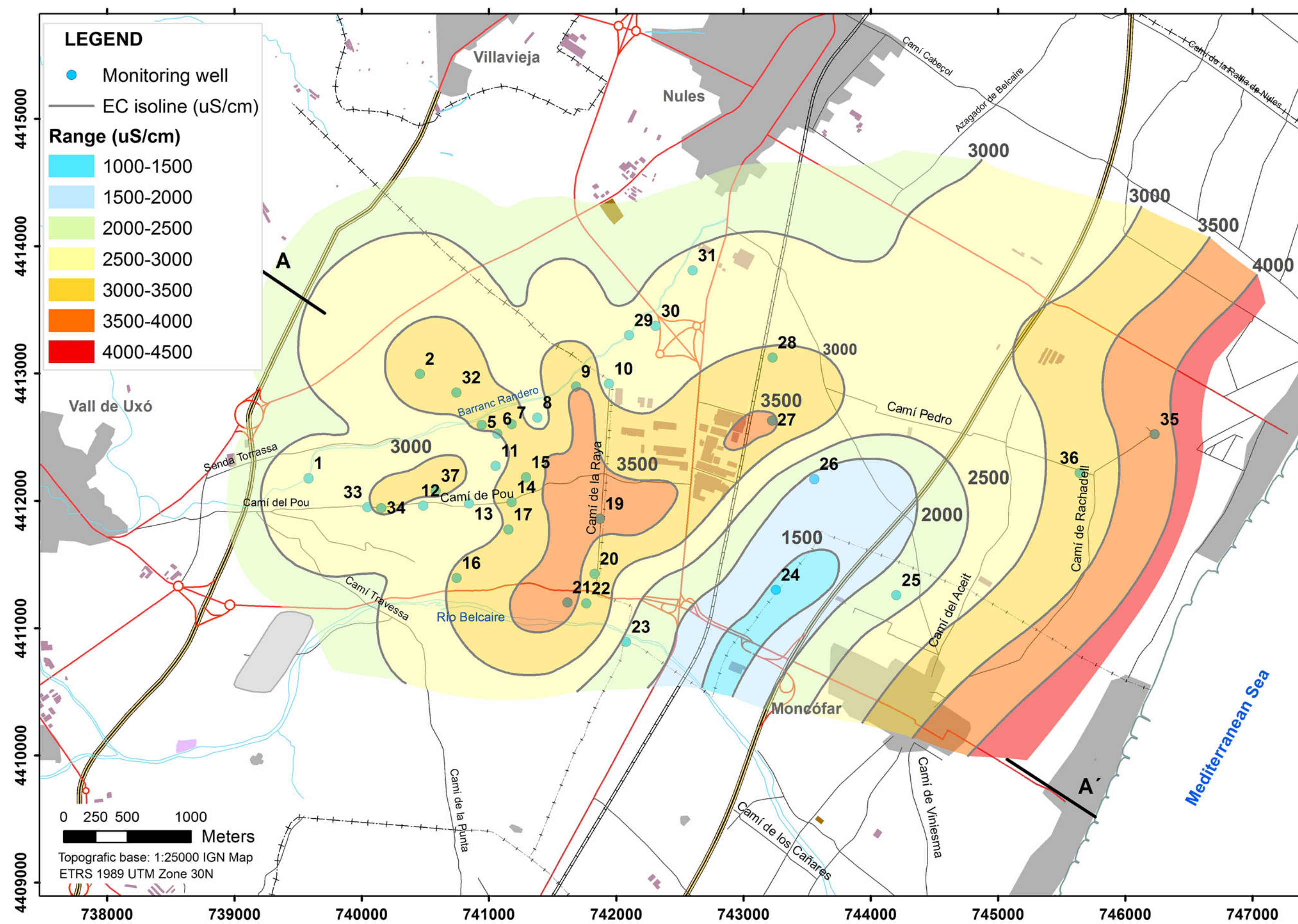

Fig. 12 Spatial distribution of electrical conductivity at 0 m a.s.l. (December 2013)

intermediate band of fresh water is narrower and minimum EC values exceed 2000 µS/cm. Likewise, in the coastal strip, the water is more saline (up to 4000 µS/cm).

The EC values at 10 m b.s.l. exceed 4500 µS/cm along the coastal strip (Fig. 14), but are generally between 3000 and 4000 µS/cm in most of the study area. It is worth noting that the inland zone with high salinity does not exactly correspond with the Rambleta area, but is slightly displaced to the east, probably because the saline front has moved towards the sea.

Finally, at 15 m b.s.l. (Fig. 15), the areas with EC values above 4000 µS/cm are linked, and extend from the coast to the Rambleta Area. Figure 15 highlights the elevated and roughly homogeneous salinity in the deeper part of the aquifer.

The geometry of the salt body reconstructed from Figs. 12, 13, 14, and 15, clearly shows that there is an area of higher salinity in the Rambleta (Fig. 16). We added a hydrogeochemical cross-section (A–A′) to represent the shape of the seawater intrusion (Fig. 16). The horizontal advance of saline water moving inland from the sea and the vertical upconing in the Rambleta Area are clearly visible. There are two saline cones, a principal cone and a secondary cone. This suggests that the saline cone was broader and is now moving towards the sea, which is consistent with the end of the groundwater exploitation at Wells 6 and 32 in the central part of the Rambleta. Conversely, the persistence of the secondary saline cone could be related to the pumping that continues in the western boundary (Well 2).

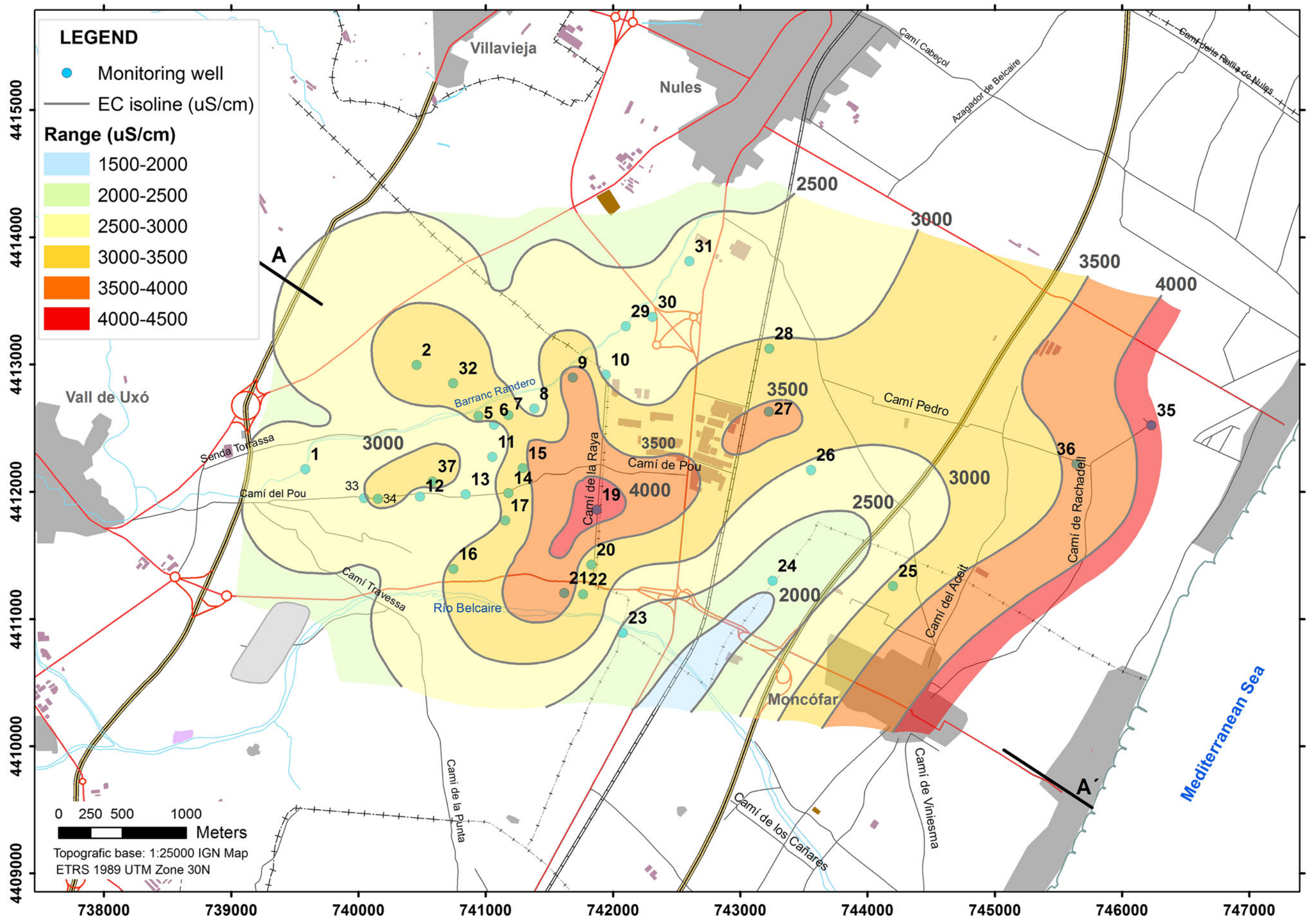

Fig. 13 Spatial distribution of electrical conductivity at depth 5 m b.s.l. (December 2013)

Conclusions

We used historical and recent data from a dense monitoring network to accurately define the geometry of the seawater intrusion at the study site. We reconstructed the dynamics of seawater intrusion and the development of upconing from historical chloride concentrations and piezometric measurements.

Because we used historical data, we had to take a number of methodological precautions; for example, we needed information about the construction characteristics of the wells (construction depth, depth into the aquifer, grids situation), and we assessed the representativeness of the samples based on the collection method. It should be noted that, where the salinity is high, piezometric corrections should be applied to account for differences in the density of water.

We evaluated the influence of the recharge and exploitation regimes on the fresh water–saline water balance by studying the development of the chloride concentrations and groundwater levels over a period of 42 years.

The dry periods that frequently occur in Mediterranean climates and the consequent increases in pumping cause severe declines in piezometric levels and progression of the saline front. Conversely, wet periods tend to restore the situation. This is the expected response, and can be applied to aquifers with similar characteristics. However, in this case, the normal situation has been made more complex by the ongoing groundwater exploitation. Dry and wet periods

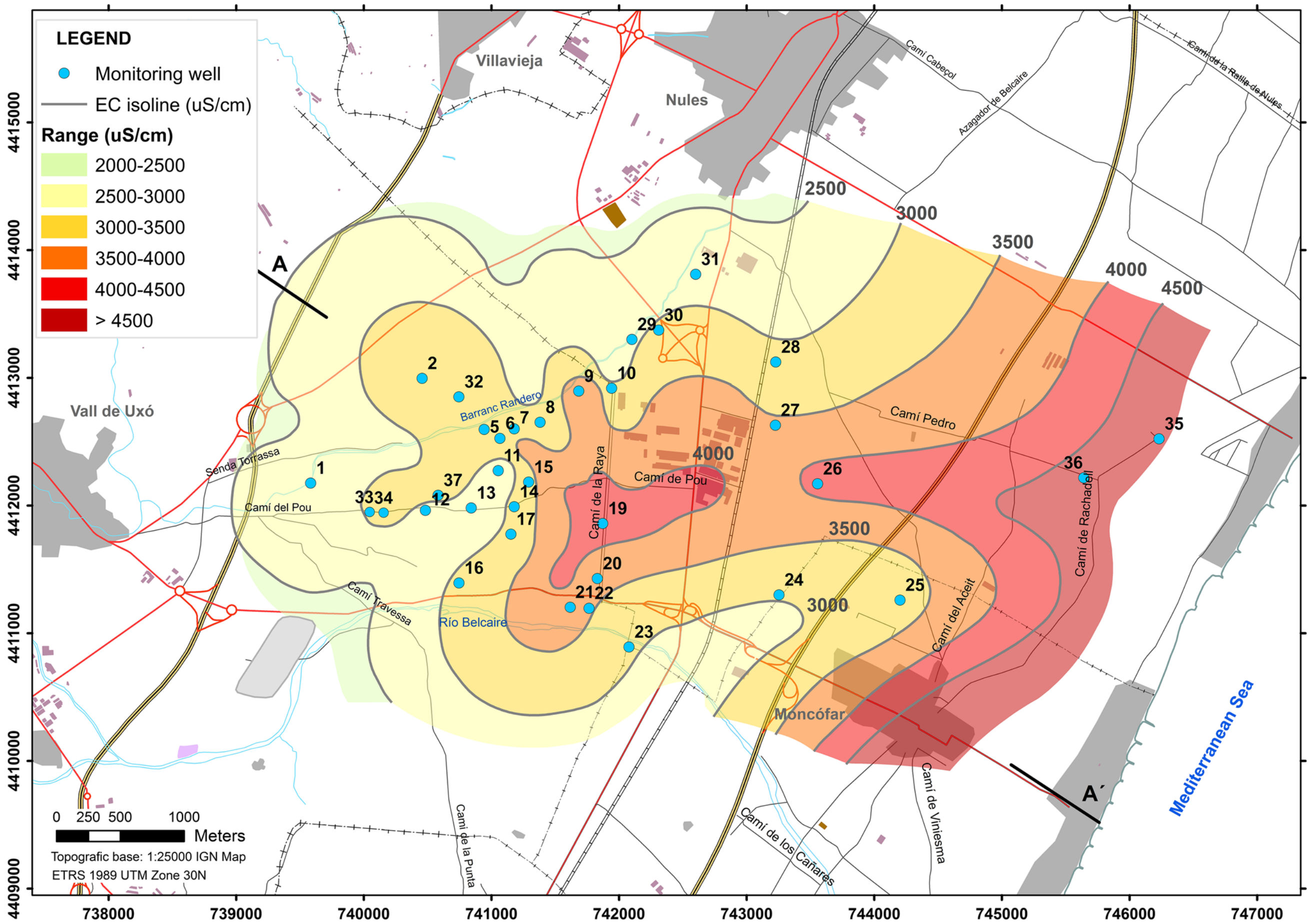

Fig. 14 Spatial distribution of electrical conductivity at depth 10 m b.s.l. (December 2013)

occurred regularly over the period when there were intensive changes in the pumping regime. During the first half of the study period (1972–1995) pumping continually increased from 10×10^6 to 24×10^6 m^3/year, while in the second half, pumping gradually decreased from a maximum of 24×10^6 to 14×10^6 m^3/year.

Chloride contour maps for different dates have shown how salinity has developed in different parts of the study site and have indicated higher chloride concentrations in the Rambleta, the area of most intense pumping. They have also allowed us to follow the emergence of an upconing process in the early 90s and the subsequent retreat of the saline front toward the coast. However, the movement of the saline cone is slow and the recovery is subject to the variable climate regime and the still significant pumping in the area.

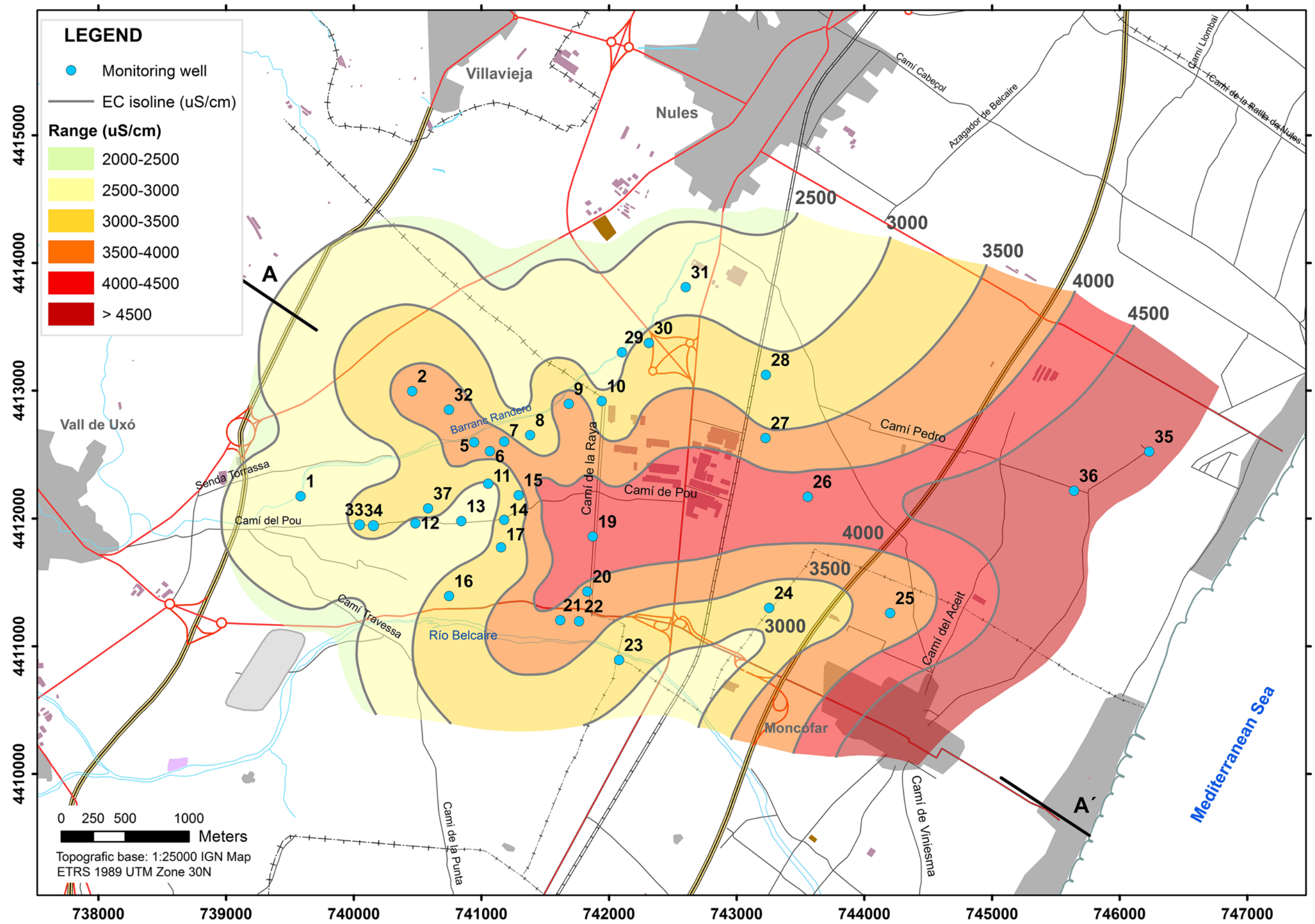

Fig. 15 Spatial distribution of electrical conductivity at depth 15 m b.s.l. (December 2013)

Thirty four vertical logs were made of EC (December 2013) to characterize the 3D nature of the saline cone. Our results show that this method can be used to effectively determine the geometry of the upconing process.

The balance of the saline front is unstable and is strongly affected by boundary conditions (pumping regime and variations in recharge). An adequate observation network should be established to ensure that EC profiles can

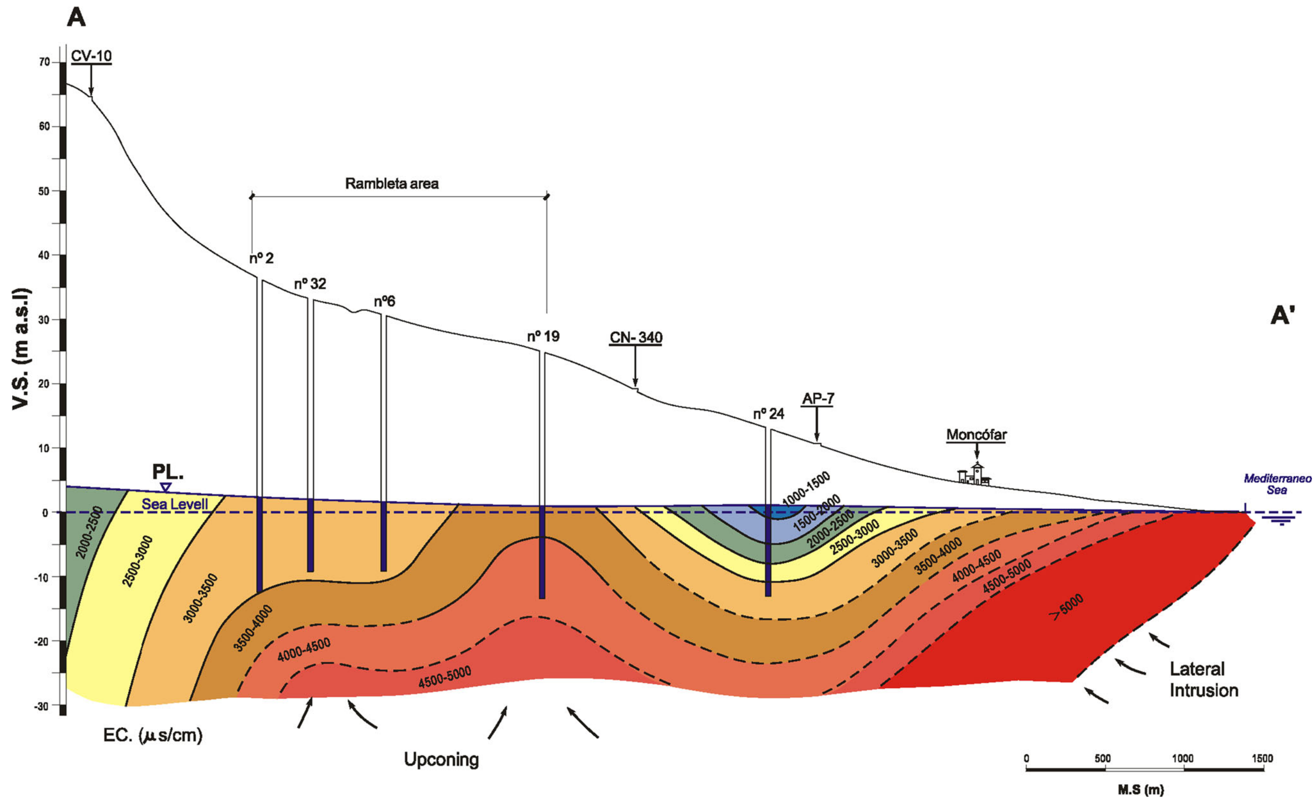

Fig. 16 Hydrogeochemical cross-section A–A′ (December 2013)

be recorded at least every 6 months on an ongoing basis in such areas.

Acknowledgments This study formed part of the project Facing seawater intrusion recharging coastal aquifers with regenerated water, financed by The Coca-Cola Foundation (Atlanta, USA), with the support of Coca-Cola Iberian Partners.

References

Aliewi AS, Mackay R, Jayyousi A, Nasereddin K, Mushtaha A, Yaqubi A (2001) Numerical simulation of the movement of saltwater under skimming and scavenger pumping in the Pleistocene Aquifer of Gaza and Jericho areas, Palestine. Transp Porous Media 43:195–212

Barlow PM, Reichard EG (2010) Saltwater intrusion in coastal regions of North America. Hydrogeol J 18:247–260. doi:10.1007/s10040-009-0514-3

Barrocu G (2003) Seawater intrusion in the coastal aquifers of Italy. In: Calaforra J (ed) State of seawater intrusion in coastal aquifers of the Mediterranean Coast. SWIM-SWICA, Alicante

Boschetti T, González-Hernández P, Hernández-Díaz R, Naclerio G, Celico F (2015) Seawater intrusion in the Guanahacabibes Peninsula (Pinar del Río Province, western Cuba): effects on karst development and water isotope composition. Environ Earth Sci 73:5703–5719. doi:10.1007/s12665-014-3825-1

Bouderbala A (2015) Groundwater salinization in semi-arid zones: an example from Nador plain (Tipaza, Algeria). Environ Earth Sci 73:5479–5496. doi:10.1007/s12665-014-3801-9

Bower JW, Motz LH, Durden DW (1999) Analytical solution for determining the critical condition of saltwater upconing in a leaky artesian aquifer. J Hydrol 221(1–2):43–54

Cai J, Taute T, Schneider M (2014) Saltwater upconing below a pumping well in an inland aquifer: a theoretical modeling study on testing different scenarios of deep saline-groundwater pathways. Water Air Soil Pollut 225:2203. doi:10.1007/s11270-014-2203-7

Cardoso PR (1993) Saline water intrusion in Mexico. Transactions on ecology and the environment, 2nd edn. WIT, Southampton. doi:10.2495/WP930051

Chandler RL, McWorther DB (1975) Upconing of the salt-water–fresh-water interface Veneta a dumping well. Groundwater 13(4):354–359

Cheng AH, Ouazar D (2003) Coastal aquifer management-monitoring, modeling, and case studies. CRC Press, Boca Raton

Custodio E (2010) Coastal aquifers in Europe: an overview. Hydrogeol J 18(1):269–280

Dagan G, Zeitoun DG (1998) Free-surface flow toward a well and interface upconing in stratified aquifers of random conductivity. Water Resour Res 34(11):3191–3196. doi:10.1029/98wr020039

Diersch HJ, Prochnow D, Thiele M (1984) Finite-element analysis of dispersion-affected saltwater upconing below a pumping well. Appl Math Model 8:305–312

Escrig I, Morell I, López FJ (1993) Estudio sobre la relación entre el contenido de metales pesados (Cd, Co y Pb) y la salinización en las aguas subterráneas de la Plana de Castellón. Aplicación de Análisis de Componentes Principales (A.C.P.) (Study of the relationship between the content of heavy metals (Cd, Co and Pb) and groundwater salinization in Plana de Castellón aquifer. Application of Principal Component Analysis). Hidrogeología 1993:19–34

FAO (1997) Seawater intrusion in coastal aquifers. Guidelines for study, monitoring and control **(ISBN: 92-5-103986-0)**

Fidelibus MD, Giménez E, Morell I, Tulipano L (1992) Salinization processes in the Castellón Plain aquifer. Custodio E, Galofre (eds) Study and modelling of salt water intrusion into aquifers. In: Proceedings of the 12th saltwater intrusion meeting, Barcelona, Spain, pp 267–284

Fleury P (2005) Sources sous-marines et aquifères karstiques côtiers méditerranéens. Fonctionnement et caractérisation. Dissertation, Université de Paris

García-Menéndez O, Renau-Pruñonosa A, Morell I, Ballesteros BJ (2015) Hydrogeochemical and hydrodynamic effects in an artificial recharge experience in a salinized coastal aquifer (Vall de Uxó, Spain). 42nd IAH congress, hydrogeology: back to the future, 13–18 September 2015, Rome, Italy. https://www.aqua2015.com/cms/uploads/pdf/abstract_712-aqua2015.pdf. Accessed 8 Apr 2016

Garabedian SP (2013) Estimation of salt water upconing a steady-state solution for partial completion of pumped well. Groundwater 51(6):927–934

Giménez E (1994) Caracterización hidrogeoquímica de los procesos de salinización del acuífero detrítico costero de la Plana de Castellón (Hydrogeochemical characterization of the salinization processes in coastal aquifer of Castellón Plain). Dissertation, Universidad de Granada

Giménez E, Morell I (2008) Contributions of boron isotopes to understanding the hydrogeochemistry of the coastal detritic aquifer of Castellón Plain, Spain. Hydrogeol J 16:547–557. doi:10.1007/s10040-008-0290-5

Giménez-Forcada E, Vega-Alegre M (2015) Arsenic, barium, strontium and uranium geochemistry and their utility as tracers to characterize groundwaters from the Espadán-Calderona Triassic Domain, Spain. Sci Total Environ 512–513:599–612

Gómez JD, López JA, Garrido E (2003) The state of seawater intrusion in Spain. IGME (ed) Coastal aquifers intrusion technology, Madrid, pp 169–185

Günay G (2003) Seawater intrusion in coastal aquifers of the Mediterranean coast of Turkey. IGME (ed) Coastal aquifers intrusion technology, Madrid, pp 265–277

Khairy H, Janardhana MR (2013) Hydrogeochemical features of groundwater of semi-confined coastal aquifer in Amol-Ghaemshahr plain, Mazandaran Province, Northern Iran. Environ Monit Assess 185:9237–9264. doi:10.1007/s10661-013-3248-6

Kouzana F, Mammou AB, Felfoul MS (2009) Seawater intrusion and associated processes: case of the Korba aquifer (Cap-Bon, Tunisia). C R Geoscience 341:21–35. doi:10.1016/j.crte.2008.09.008

Kura NU, Ramli MF, Ibrahim S, Sulaiman WNA, Zaudi MA, Aris AZ (2014) A preliminary appraisal of the effect of pumping on seawater intrusion and upconing in a small tropical island using 2D resistivity technique. Sci World J:11 **(ID 796425)**

Lambrakis N, Marinos P (2003) The salinization of coastal aquifers in Greece; a general review. IGME (ed) Hidrogeología y Aguas Subterráneas 8. Coastal aquifers intrusion technology: Mediterranean countries, Madrid, pp 251–263

Liu D (2004) The situation and analysis of salinity intrusion in coastal areas, China. J Geol Hazards Environ Preserv. doi:10.1007/s12665-014-3186-9

Marandi A, Vallner L (2010) Upconing of saline water from the crystalline basement into the Cambrian-Vendian aquifer system on the Kopli Peninsula, northern Estonia. Est J Earth Sci 59(4):277–287. doi:10.3176/earth.2010.4.04

Mondal NC, Singh VP, Singh S, Singh VS (2011) Hydrochemical characteristics of coastal aquifer from Tuticorin, Tamil Nadu, India. Environ Monit Assess 175(1–4):531–550

Morell I, Ballesteros BJ, García O, Renau-Pruñonosa A, Renau-Llorens A, Rosado S (2014) Water recovery project: the first experience of deep injection in Castellón, Spain. Results of the first phase and next steps. DEMEAU Workshop on Managed Aquifer Recharge and Emerging Micropollutants. Barcelona, Spain. http://demeau-fp7.eu/events/266

Morell I, Giménez E, Esteller MV (1996) Application of principal components analysis to the study of salinization of the Castellon Plain (Spain). Sci Total Environ 177:161–171

Morell I, Giménez E, Fagundo JR, Pulido-Bosch A, López-Chicano M, Calvache ML, Rodríguez JE (1997) Hydrochemistry and karstification in the Cienaga de Zapata aquifer (Matanzas, Cuba). In: Günay, Johnson (eds) Karst waters and environmental impacts. Balkema, Rotterdam, pp 191–198

Motz LH (1992) Salt-water upconing in an aquifer overlain by a leaky confining bed. Groundwater 30(2):192–198

Oswald SE, Scheidegger MB, Kinzelbach W (2002) Time-dependent measurement of strongly density-dependent flow in a porous medium via nuclear magnetic resonance imaging. Transp Porous Media 47:169–193

Paniconi C, Khlaifi I, Lecca G, Giacomelli A, Tarhouni J (2001) Modeling and analysis of seawater intrusion in the coastal aquifer of eastern Cap-Bon, Tunisia. Transp Porous Media 43:3–28

Parck Y, Lee JY, Kim JH, Song SH (2012) National scale evaluation of groundwater chemistry in Korea coastal aquifers: evidences of seawater intrusion. Environ Earth Sci 66:707–718. doi:10.1007/s12665-011-1278-3

Paster A, Dagan G (2008) Mixing at the interface between fresh and salt waters in 3D steady flow with application to a pumping well in a coastal aquifer. Adv Water Resour 31:1565–1577. doi:10.1016/j.advwatres.2008.06.008

Petalas C, Lambrakis N (2006) Simulation of intense salinization phenomena in coastal aquifers—the case of the coastal aquifers of Thrace. J Hydrol 324:51–64

Post V, Kooi H, Simmons C (2007) Using hydraulic measurements in variable-density ground water flow analyses. Groundwater 45(6):664–671. doi:10.1111/j.1745-6584.2007.00339.x

Pratheepa V, Ramesh S, Sukumaran N, Murugesan AG (2015) Identification of the sources for groundwater salinization in the coastal aquifers of Southern Tamil Nadu, India. Environ Earth Sci 74:2819–2829. doi:10.1007/s12665-015-4303-0

Reilly TE, Frimpter MH, LeBlanc DR, Goodman AS (1987) Analysis of steady-state saltwater upconing with the application at Truro well field, Cape Cod, Massachusetts. Groundwater 25(2):194–206

Reilly TE, Goodman AS (1987) Analysis of saltwater upconing beneath a pumping well. J Hydrol 89(3–4):169–204

Renau-Llorens EA (2010) Elementos minoritarios y traza en la masa de agua subterránea 080.021 (Plana de Castelló). Origen y procesos asociados (Minor and trace elements in the groundwater body 080.021 (Plana de Castelló). Origin and associated processes). Dissertation, Universitat Jaume I

Rey J, Martínez J, Barberá GG, García-Arostegui JL, García-Pintado J, Martínez-Vicente D (2013) Geophysical characterization of the complex dynamics of groundwater and seawater exchange in a highly stressed aquifer system linked to a coastal lagoon (SE Spain). Environ Earth Sci 70:2271–2282. doi:10.1007/s12665-013-2472-2

Steyl G, Dennis I (2010) Review of coastal-area aquifers in Africa. Hydrogeol J 18:217–225. doi:10.1007/s10040-009-0545-9

Stoecker F, Babel MS, Das Gupta A, Rivas AA, Evers M, Kazama F, Nakamura T (2013) Hydrogeochemical and isotopic characterization of groundwater salinization in the Bangkok aquifer system, Thailand. Environ Earth Sci 68(3):749–763

Vengosh A, Spivack AJ, Artzi Y, Ayalon (1999) Boron, strontium and oxygen isotopic and geochemical constraints for the origin of the salinity in ground water from the Mediterranean coast of Israel. Water Resour Res 35:1877–1894

Werner AD, Habermehl MA, Laity T (2005) An Australian perspective of seawater intrusion. 2nd Int. Salinity Forum. Salinity, water and society-global issues, local action

Werner AD, Jakovovic D, Simmons CT (2009) Experimental observations of saltwater up-coning. J Hydrol 373:230–241. doi:10.1016/j.jhydrol.2009.05.004

Werner AD, Bakker M, Post VEA, Vandenboede A, Lu CH, Ataie-Ashtiani B, Simmons CT, Barry DA (2013) Seawater intrusion processes, investigation and management. Recent advances and futures challenges. Adv Water Resour 51:3–26

Wirojanagud P, Charbeneau RJ (1985) Saltwater upconing in unconfined aquifers. J Hydraul Eng 111(3):417–434

Zakhem BA, Hafez R (2007) Environmental isotope study of seawater intrusion in the coastal aquifer (Syria). Environ Geol 51:1329–1339

Zhou Q, Bear J, Bensabat J (2005) Saltwater upconing and decay beneath a well pumping above an interface zone. Transp Porous Media 61:337–363. doi:10.1007/s11242-005-0261-4